Modeling Dynamic Ice Loss on The Greenland Ice Sheet Using Satellite Data

Betsy McCall

SCI 489

Southern New Hampshire University

October 2024

Introduction (Statement of the Problem)

This analysis brings together several datasets for exploration. The primary dataset is described in Csatho, et al. (2014). She and her colleagues bring together the data from several NASA laser altimetry missions obtained via satellite and some airborne overflights. These datasets are combined and processed together to provide predictions for 1-km^2 patches of the Greenland Ice Sheet (GrIS) for elevation. The data is further processes to extract known factors that contribute to variations in height such as snowfall and snowmelt, firn compaction, crustal rebound, etc., leaving behind an estimate for how the ice thickness is changing over time. Since the 2014 article, the dataset has been extended to include through the end of the ICESat-1 mission in spring of 2017, these tiles cover the time frame 1994 to 2017. The dataset also contains reference elevation (as of 2006) which will also be modeled as part of this analysis. Figure 1 (bottom image) shows the regions to be analyzed (full maps of Greenland from which these were taken are included in the Appendix as Figure 1A). Figure 2 shows the map of Greenland with red dots overlaid for each location a time series occurs in the Csatho dataset.

In addition, for comparison, the data will be compared to Greenland drainage basins (Mouginot & Rignot, 2019) to determine if ice loss patterns align with expectations from drainage basin flow speeds. Figure 1 (top image) shows the region of analysis (the full map of Greenland is included in the Appendix as Figure 2A). All the analysis presented here was done in the R programming language unless otherwise noted.

The question being asked is to what extent the dynamic ice loss is associated with geographical features such as elevation, and drainage basins, or other environmental phenomena such as ice velocity flow speeds on the Greenland ice sheet.

Exploratory Data Analysis

In preparation for modeling, a brief analysis of the dataset was undertaken to determine what cleaning might have to be done prior to modeling. The initial statistical summary of the dynamic ice loss variable is shown in the Table 1.

Figure 1. The image shows the regions in Greenland to be analyzed in the northern-most portion of Greenland, the locations of Tiles 30-36 from the Csatho dataset and the Mouginot & Rignot drainage basins. The brown dots in the top image are glacier outlets. The blue dots in the bottom image are also glacier outlets. The high flow areas in the top image are in dark blue, while lower flow basins are in light blue. The red lines mark the bounding boxes of the Tiles in the Csatho dataset.

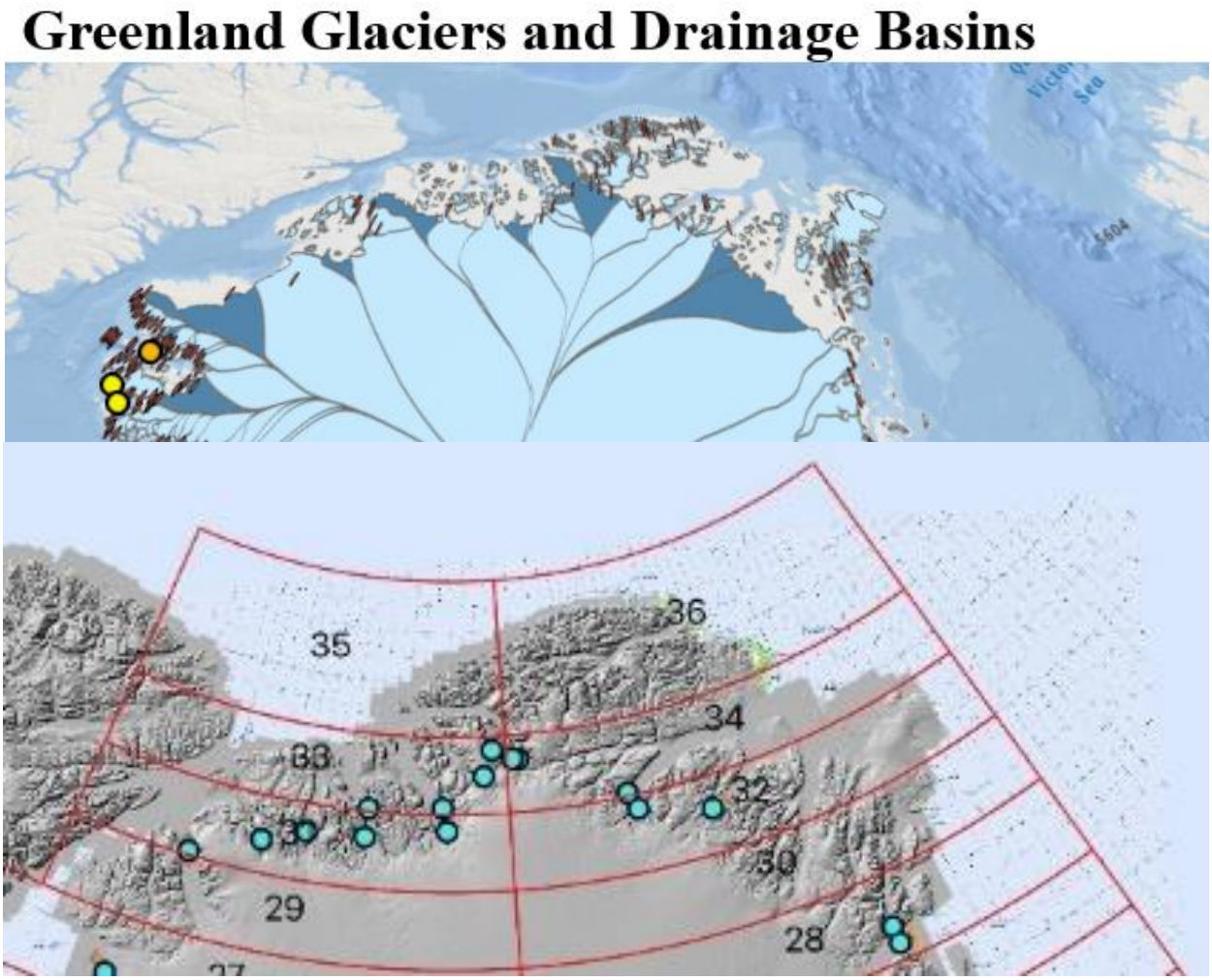

Table 1. A statistical summary table of the dynamic ice loss variable from the Csatho dataset on Tiles 30-36, in meters.

Min.	1st Qu.	Median	Mean	3rd Qu.	Max.	St.Dev.
-14634.129	0.032	0.469	0.284	1.477	6006.761	84.358

As one can see from the data, the middle half of the dataset only spans a range of 1.445 m, while the minimum and maximum values are a hundred times that size. While the standard deviation is affected by the presence of such extreme outliers, the minimum is 173 standard deviation from the mean, while the maximum is 71 standard deviations from the mean. Given the size of the dataset on these tiles of 66,195 observations, this size of extreme outliers is highly unlikely due to just random chance. Given the general limitations of laser altimetry data on steep-sloped terrain (Csatho, Schenk, Veen, & Angelen, 2014), it's highly likely that these outcomes are derived from measurement errors. Indeed, the depth of the Greenland ice sheet is around 3 km, a gain of 6 km (the maximum) or a loss of 14 km (minimum) is physically impossible. In an effort to err on the size of conservatively keeping as many values as possible, however, a determination was made to trim the data around the 5^{th} standard deviation from the mean (approximately $\pm$400 m based on the initial statistics). One would expect that some extreme values would exist in the data just due to random chance, but this trim would remove the most obviously erroneous values, while still maintaining the possibility of limiting the reduction of statistical variability. The data is not normally distributed, so maintaining some relatively large outliers should also serve to maintain the character of the distribution. The statistical summary of the remaining data after trimming the most extreme outliers is shown in Table 2. Forty observations were removed in the trimming, leaving 66,155 observations. Based on the new statistics, the extremes are approximately 40 standard deviations from the mean (based on the

new standard deviation), but the distribution is more symmetrical and this is still less extreme than before trimming. As shown in Figure 3, trimming the limits of the graphical representations of the data will be further necessary to examine the majority of the data contained in a much more tightly constrained range of values.

Table 2. A statistical summary table of the dynamic ice loss variable from the Csatho dataset on Tiles 30-36, in meters, after removing all values that exceeded $\pm 400\ m$.

Min.	1st Qu.	Median	Mean	3rd Qu.	Max.	St. Dev.
-374.6760	0.0320	0.4690	0.8058	1.4765	388.6700	9.397934

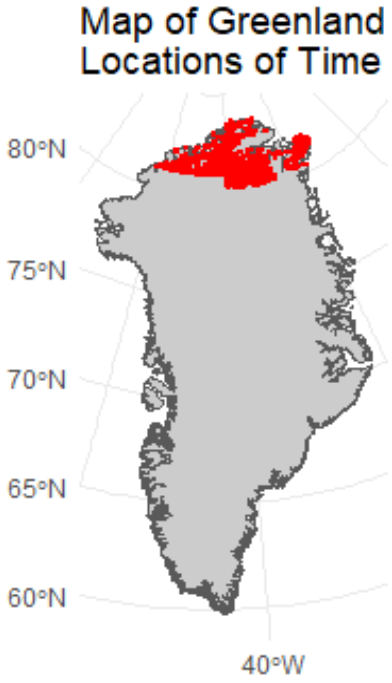

Figure 2. This image shows the full map of Greenland in stereographic projection. Each red dot is a location of a time series to be analyzed. Some time series in the set are as many as 39 observations in a 1-km^2 area, however, some locations have only one observation in between 1994 and 2017.

Figure 3 visualizes the majority of the data in a histogram. While some large values remain, for the distribution to be visible on the graph, the x-axis was reduced to much smaller range so that the data would not all be grouped into a single bin at the center of the graph, and other bins too small to see. Figure 4 shows a comparative box plot of the data separated by Tile, and Figure 5 shows a comparative box plot separated by year. These graphs suggest that broadly speaking, this region of Greenland appears to relatively stable, with means consistently a bit

above zero (the reference year is 2006), suggesting that the region may be losing as much ice as it gains, or else, is very slightly gaining mass. Since other research, including Csatho, et al. (2014) indicates that the island as a whole is losing mass, this is interpreted as a local effect. Table 3 shows the counts of observations on each tile by year.

In addition to looking at the dataset overall, some selected time series were examined to see the behavior in selected locations. An example time series plot is shown in Figure 6. The time series plotted is the longest time series on the selected tiles (39 observations). It appears to about what one might expect from the overall pattern of the data in Figures 3-5.

Figure 3. The graph shows a histogram of dynamic ice loss, with the x-axis trimmed to -15 to 15 m. The overwhelming majority of the data set is in this range of values. While the true distribution extends quite outside this range, the trimmed values represent less than 1% of data in Tiles 30-36.

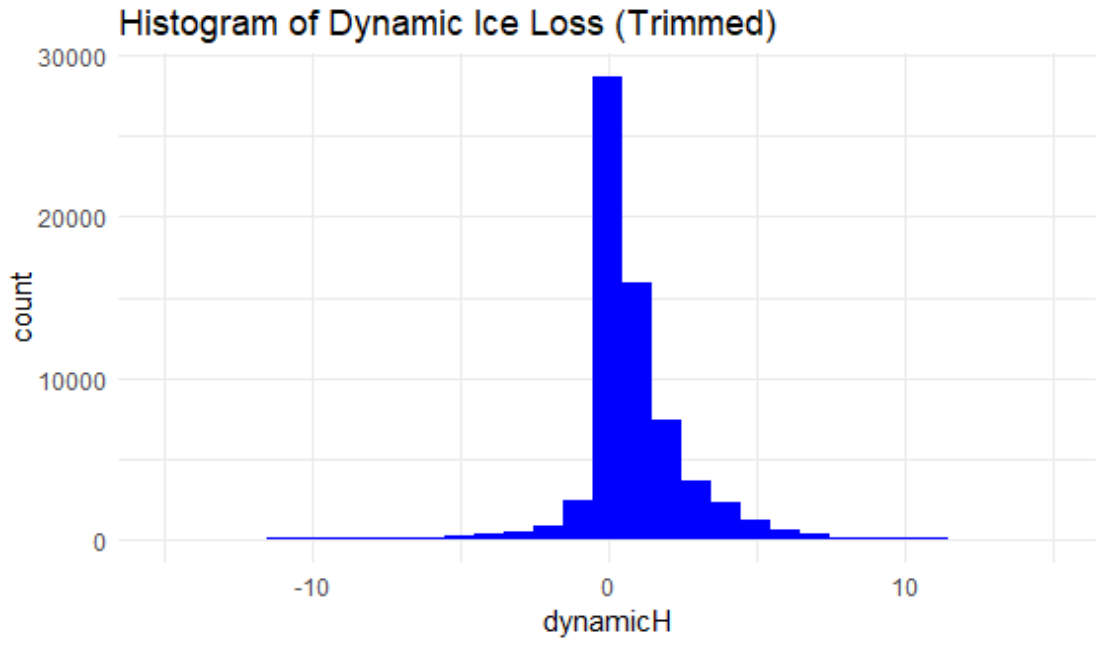

Figure 4. This graph is a comparative boxplot of the dynamic ice loss over the Tiles 30-36. As with the histogram, this x-axis has been trimmed to same range, -15 to 15 m. The tile numbers are noted on the vertical axis. As indicated by the histogram, all the tiles show a relatively small, slightly positive range, for most of the data with extreme outliers on both sides of the distribution across all regions.

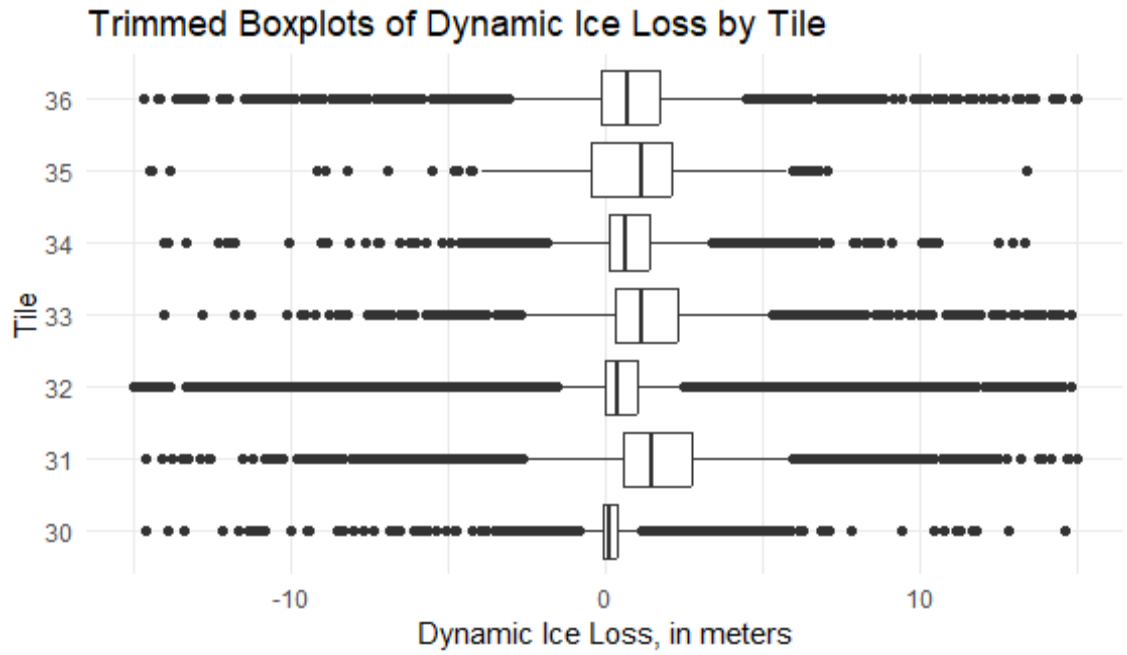

Figure 5. The comparative boxplot shows the range of the data available on Tiles 30-36 separated by year, spanning 1994 to 2017. As with the previous graphs, the x-axis has been trimmed to -15 to 15 m. The counts of observations varies greatly from year to year. The year 1996 appears to be the only year showing general loss, however, the number of observations from this year is comparatively small.

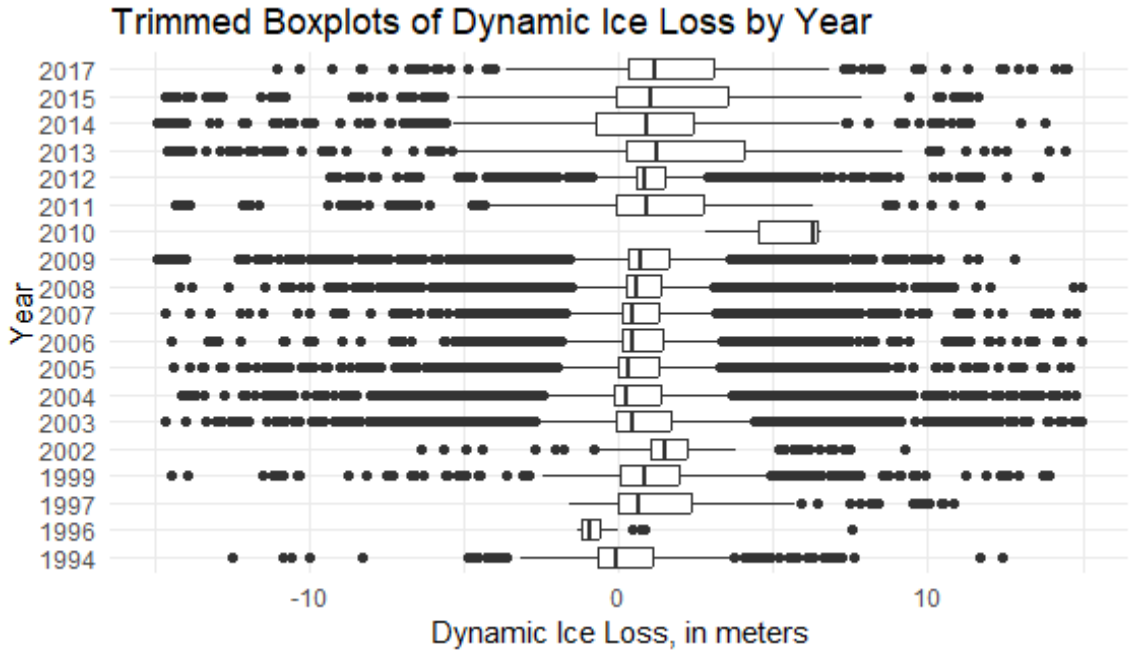

Figure 6. The plotted points in black dots are the observations from the selected time series (from Tile 31). The red curve is a LOESS interpolation of the trend indicate a slight gain in ice depth over time. The grey region is the bounds on the LOESS model error.

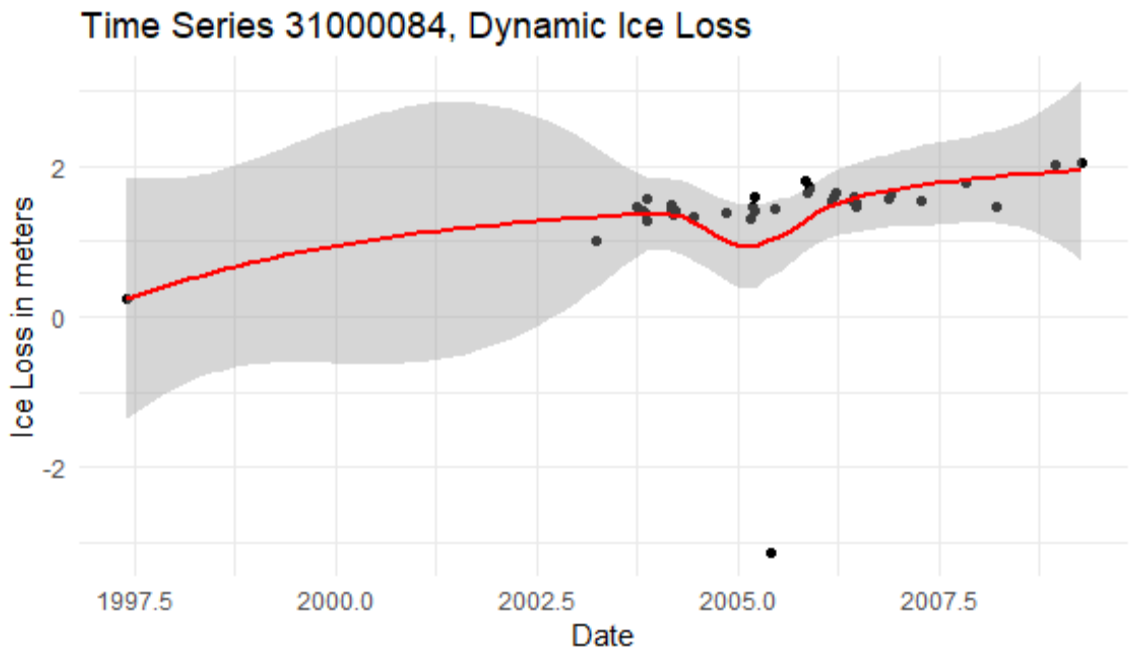

Finally, the reference elevation data was modeled to produce an elevation map of the region for comparison. Models were constructed using both LOESS and Gaussian Process Regression (kriging). These elevation models are shown in Figures 7 and 8. As you can see from the graphs, the LOESS model is much smoother, but tends to run off to large values where data is unavailable. The Gaussian process model is more responsive to local changes and produces a model with more elevation changes throughout the region. I included both types of models here since the dynamic ice loss was also modeled with both types of processes. It will be interesting to compare whether the ice loss trends are as dramatically different as the corresponding elevation models.

Figure 7. This image shows a LOESS elevation model on Tiles 30-36. Data is missing from the bottom left corner (this represents Tile 29 in the dataset which was not included) and it shows the effect of the local polynomial model tending toward infinity outside the range of local data. The elevation model was trimmed to the land area of Greenland, and the x- and y-axis values were converted from UTM-24 (in the Csatho dataset) to degrees for plotting in a stereographic projection. This model used a 30% span.

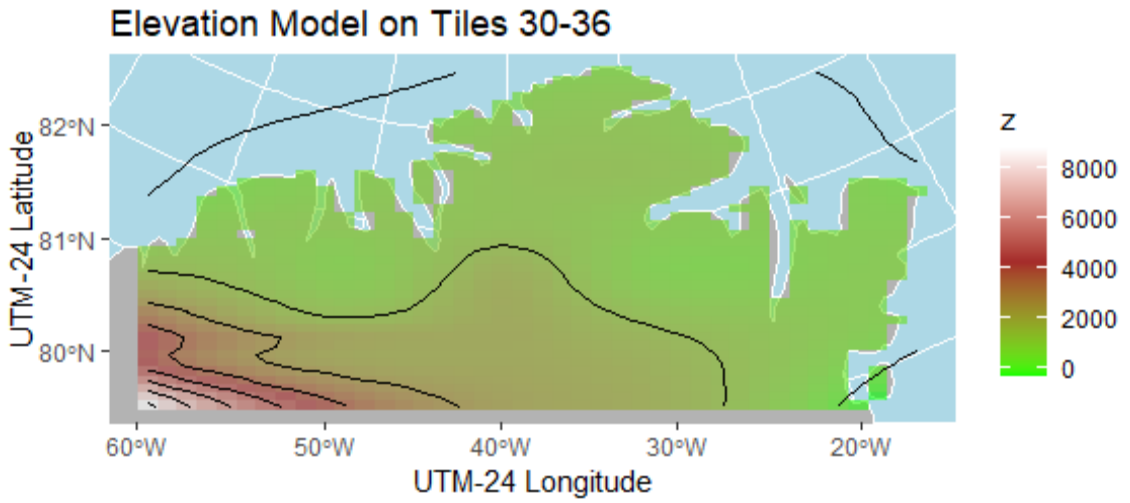

Figure 8. The Gaussian Process (kriging) model of Greenland elevation data over Tiles 30-36. This is a much more dynamic model than the LOESS model with relatively more elevation changes as it is more responsive to local changes. As with the LOESS model, the predictions were trimmed to cover only the land area of Greenland after modeling, and the coordinates converted to Stereographic projection for plotting.

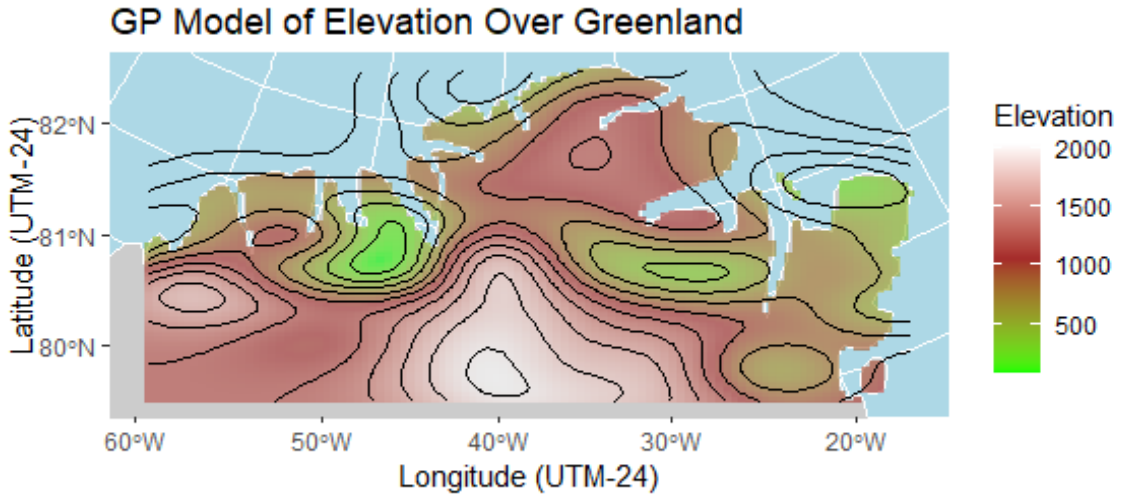

Table 3. The table shows the number of observations per tile per year. The years that have observations on every tile in the range are 2003-2009, and 2013.

Year/Tile	30	31	32	33	34	35	36
1994	110	97	169	0	3	0	0
1996	0	38	0	0	0	0	0
1997	115	125	65	7	0	0	0
1999	114	615	212	31	18	0	0
2002	0	306	0	6	0	0	0
2003	1609	2599	1991	313	340	28	301
2004	3474	3685	3125	499	499	68	495
2005	3366	2949	3104	435	462	69	500
2006	3323	2926	2983	377	430	53	434
2007	2240	1872	2068	284	339	54	270
2008	2546	1927	2213	320	367	46	367
2009	1582	1237	1554	139	186	13	126
2010	0	6	0	0	0	0	0
2011	87	186	180	8	0	0	0
2012	616	307	471	26	71	0	0
2013	89	283	227	74	2	4	49
2014	21	124	325	37	24	0	5
2015	61	116	200	13	0	0	1
2017	50	91	188	10	25	0	0

Modeling Approaches (Purpose of the Research)

To understand the dynamic ice loss (or gain) over the northern region of Greenland, the data was separated into yearly datasets (the years are noted in Figure 5's vertical axis). Not all years in the range had observations, and some of the years that did have observations only had a small number of observations from one or two tiles.

LOESS models are built from local polynomials using (in most cases) 30% of the available data from that year (some smaller years required me to use 50% because the number of observations was too small to fit a model with the preferred span). One limitation of LOESS models, is that the models constructed in most R packages supports interpolation only, not extrapolation, so models are limited to the region in which data occurs (although for the two-

dimensional model this is constrained by the minimum and maximum in x and y independently providing for a rectangular model region). The LOESS models in this analysis were created from the {tgp} package.

Gaussian process models from the {kernlab} package were used to construct the GP models of dynamic ice loss (as with the elevation models). The {kernlab} package, however, does not include uncertainty calculations for the model in the model output, so {RobustGASP} was used for some uncertainty modelling. However, {kernlab} was able to handle larger dataset than the primary GP model {RobustGASP}, so larger yearly sets had to be subdivided and retiled to obtain model errors. One advantage of Gaussian process models is that they do permit extrapolation beyond the range of the available data, and the extrapolation, unlike with a polynomial model that trends off to infinity, trends to the mean of the observations. This will be an important consideration in years where there is relatively little data to model. Years like 2010 and 1996 have particularly limited data (as shown in Table 3.)

Results of Dynamic Ice Loss Analysis (Research and Methodologies)

Models of the dynamic ice loss (relative to 2006) were constructed and a comparison of the LOESS and Gaussian process models from selected years (2003, 2008, 2013) are shown in Figures 9, 10 and 11. The LOESS model, as we saw with the elevation model, shows a more gently sloping terrain, while the Gaussian process model shows more dynamic elevation changes. Similar effects are seen in the dynamic ice loss models. In 2003, this is prior to the reference year, so positive (blue) values indicate that there was ice loss between this time and 2006, and red indicates areas that are lower in 2003 compared to 2006 and so indicate ice gain going forward in time.

Figure 12 shows the relationship between the elevation model and the dynamic ice loss from 2013, seven years after the reference elevations. Visually, there does not appear to be a strong relationship between elevation in this region and ice loss, which some low-lying regions showing gains while other low lying regions showing losses, and higher elevation regions showing more stability.

Figure 13 compares the Gaussian process model of the 2013 dynamic ice loss to the drainage basin data (Mouginot & Rignot, 2019). This visual comparison does suggest a possible relationship between faster flowing drainage basins and areas of ice loss in this region. Figure 14 shows a similar comparison with ice velocity data from (Solgaard, et al., 2021) covering the years 2016 to 2021. Both comparison such similar conclusions, that higher ice flow rates are associated geographically with areas of greater ice loss.

Figure 9. The images below show models of the dynamic ice loss from 2003. The top image shows the LOESS model, while the bottom image shows the Gaussian process model. The qualitative differences between the models mirror the qualitative differences in the elevation models, with the LOESS model being relatively smoother, while the Gaussian process model shows more local changes. In these graphs, blue is positive change (gain in ice) while red is negative change (a loss in ice). There is some reason to believe that increases in elevation are associated with ice gain, but the LOESS model shown here would appear to contract that result, however, the bottom left corner of the image is the farthest away from observations included in the model, and so the error is the largest here. The models are trimmed to cover only land area. This model is 3 years before the reference year of 2006, so blue regions would indicate loss between 2003 and 2006 (gain backwards in time). White regions are areas of stability between 2003 and 2006.

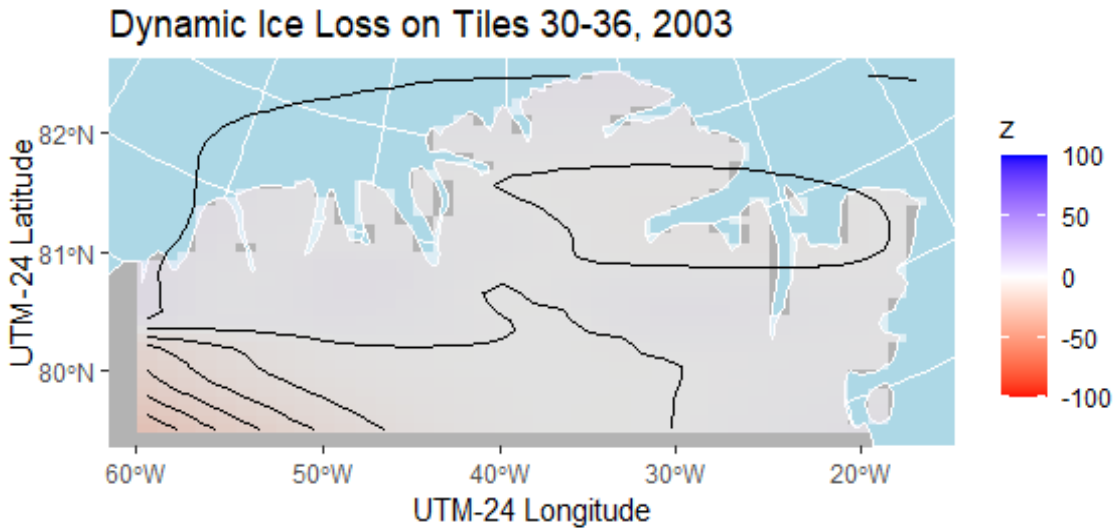
Dynamic Ice Loss on Tiles 30-36, 2003
82°N
81°N
80°N
UTM-24 Latitude
60°W
50°W
40°W
30°W
20°W
UTM-24 Longitude
Z
100
50
0
-50
-100

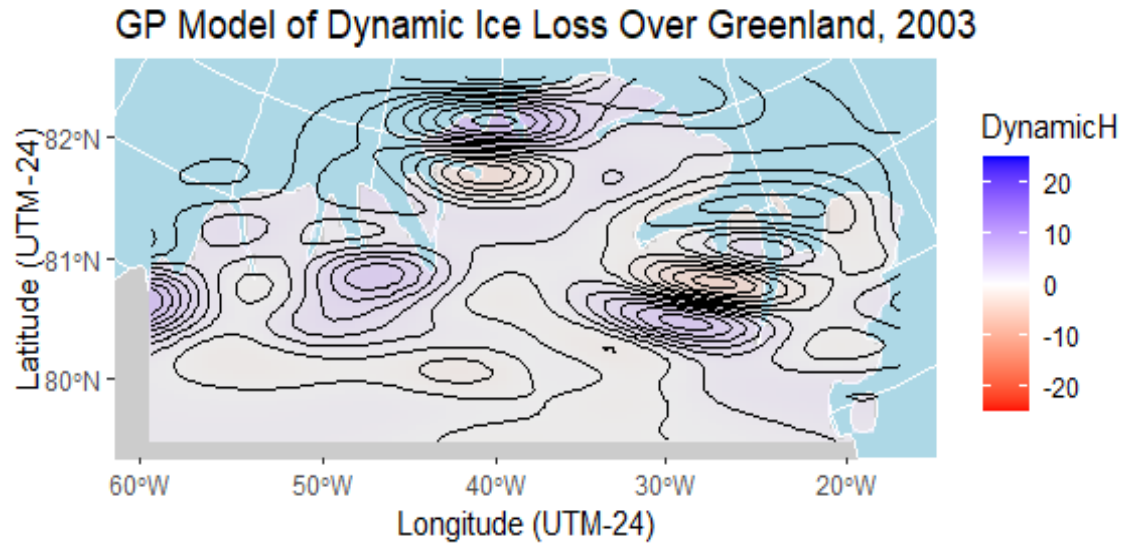
GP Model of Dynamic Ice Loss Over Greenland, 2003
82°N
81°N
80°N
Latitude (UTM-24)
60°W
50°W
40°W
30°W
20°W
Longitude (UTM-24)
DynamicH
20
10
0
-10
-20

Figure 10. The images below show models of the dynamic ice loss from 2008. The top image shows the LOESS model, while the bottom image shows the Gaussian process model. In these graphs, blue is positive change (gain in ice) while red is negative change (a loss in ice). This year represents the LOESS model with some of the more textured results compared to other model years. The models are trimmed to cover only land area. The relative change being so close to 0 in the LOESS model is sensible since this is only two years after the reference year of 2006.

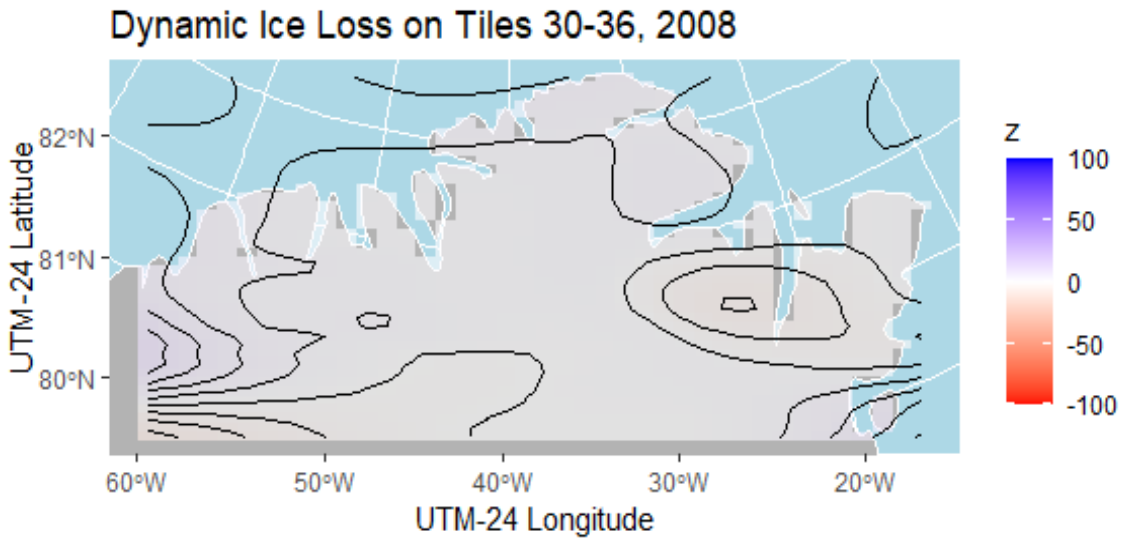

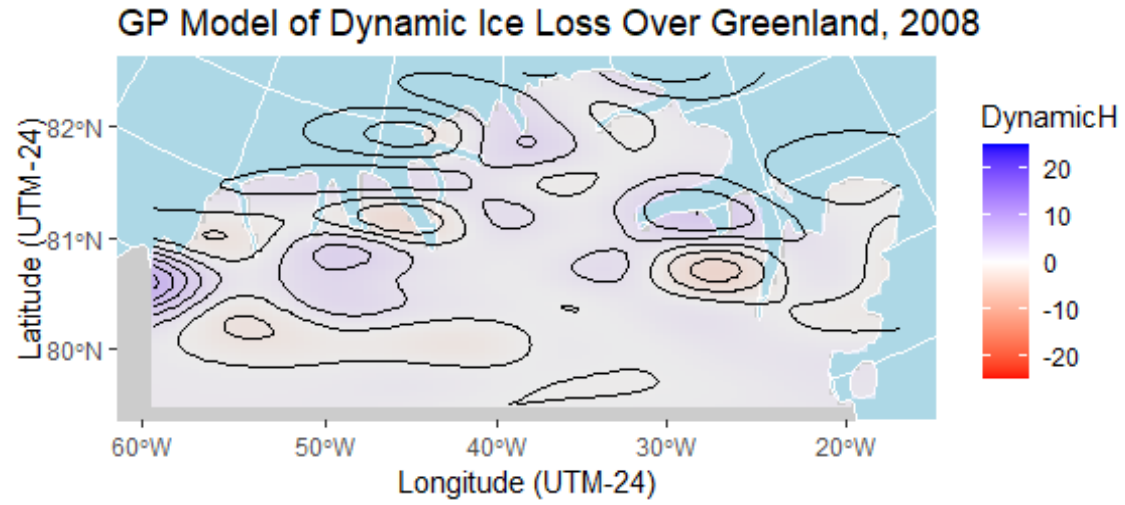

Figure 11. The images below show models of the dynamic ice loss from 2013. The top image shows the LOESS model, while the bottom image shows the Gaussian process model. In these graphs, blue is positive change (gain in ice) while red is negative change (a loss in ice). This year represents the strongest relationship between the LOESS and the Gaussian process model. The models are trimmed to cover only land area. The relatively darker regions of red and blue indicate greater change from the reference year values from 2006.

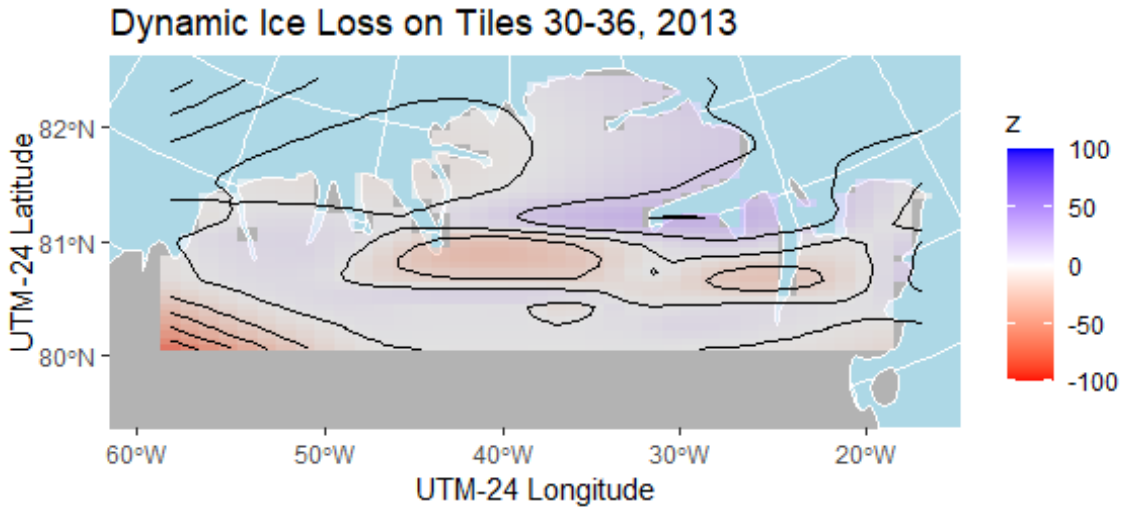

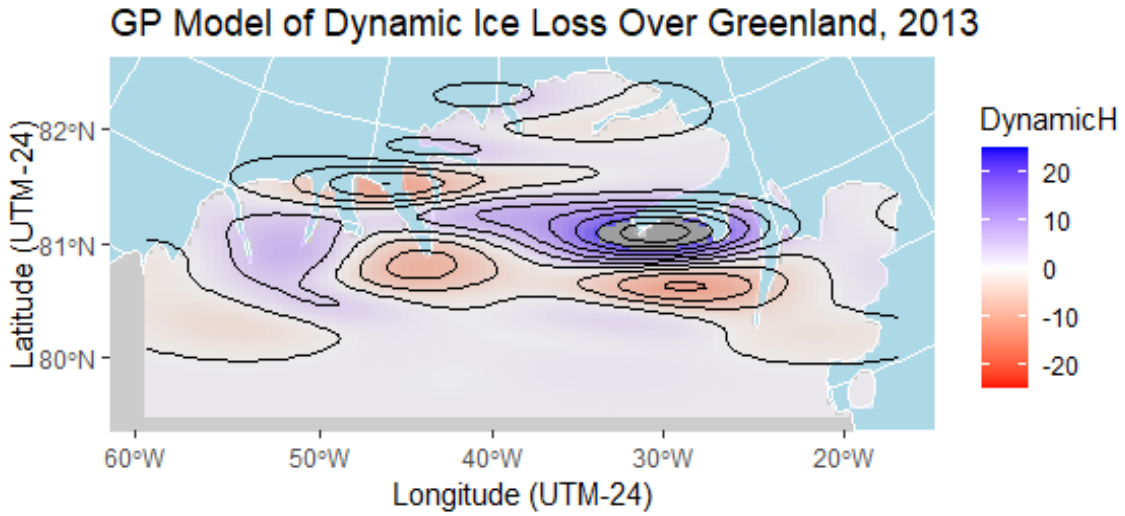

Figure 12. Comparison of the Gaussian process model of dynamic ice loss to the geographic model. There are superficial similarities between the geography and the ice loss, but they are not consistent in terms of elevations. The lower elevation region on the right (oval) corresponds to a region of ice gain, while the lower elevation level on the left corresponds to a region of ice loss.

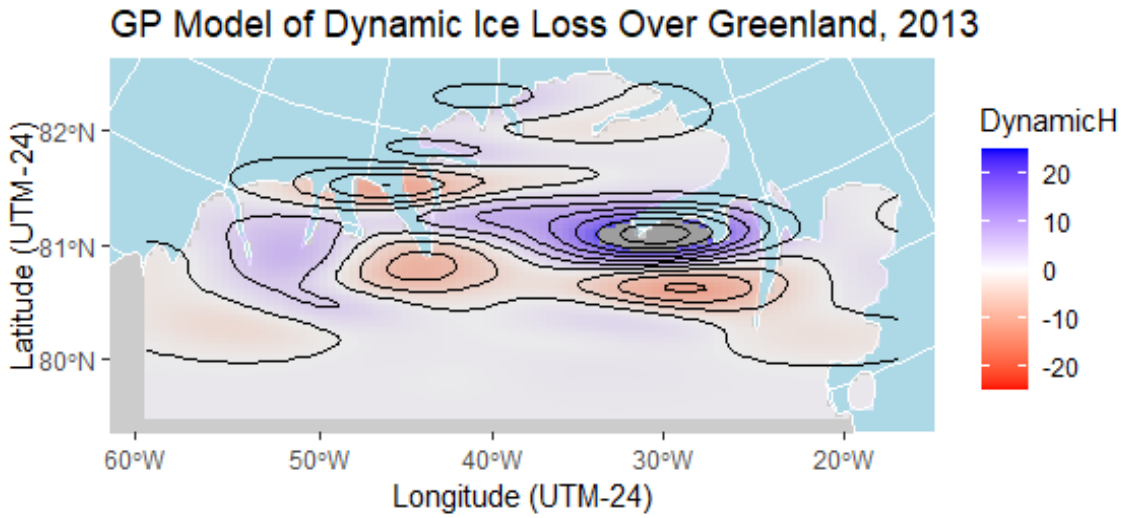

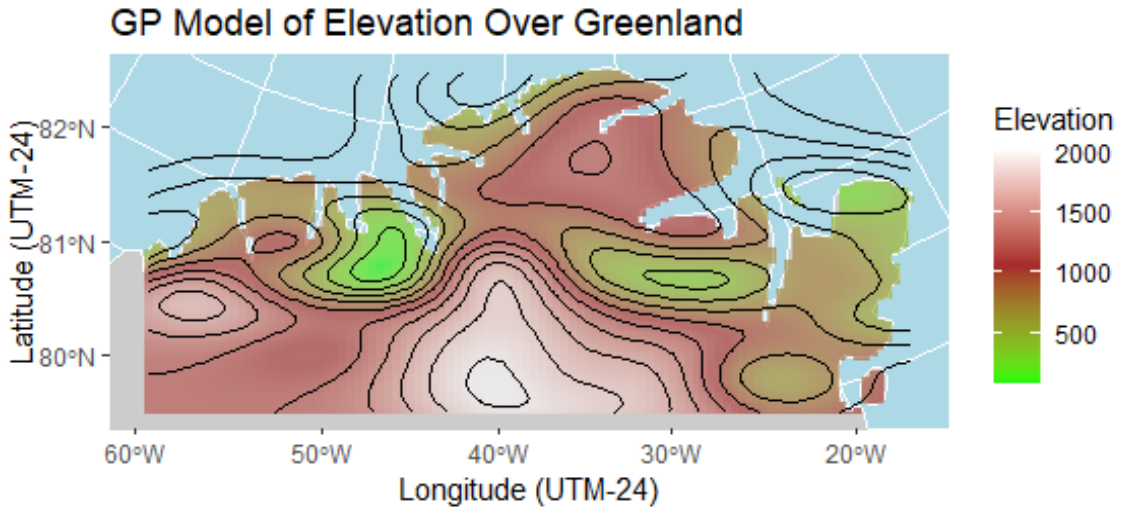

Figure 13. This figure shows the side-by-side comparison of the drainage basins and the dynamic ice loss model (Gaussian process model) from 2013. Red regions on the GP model are areas of ice loss, while the dark blue regions on the drainage basins are areas of faster flow. There does appear to be some relationship between these regions at first glance.

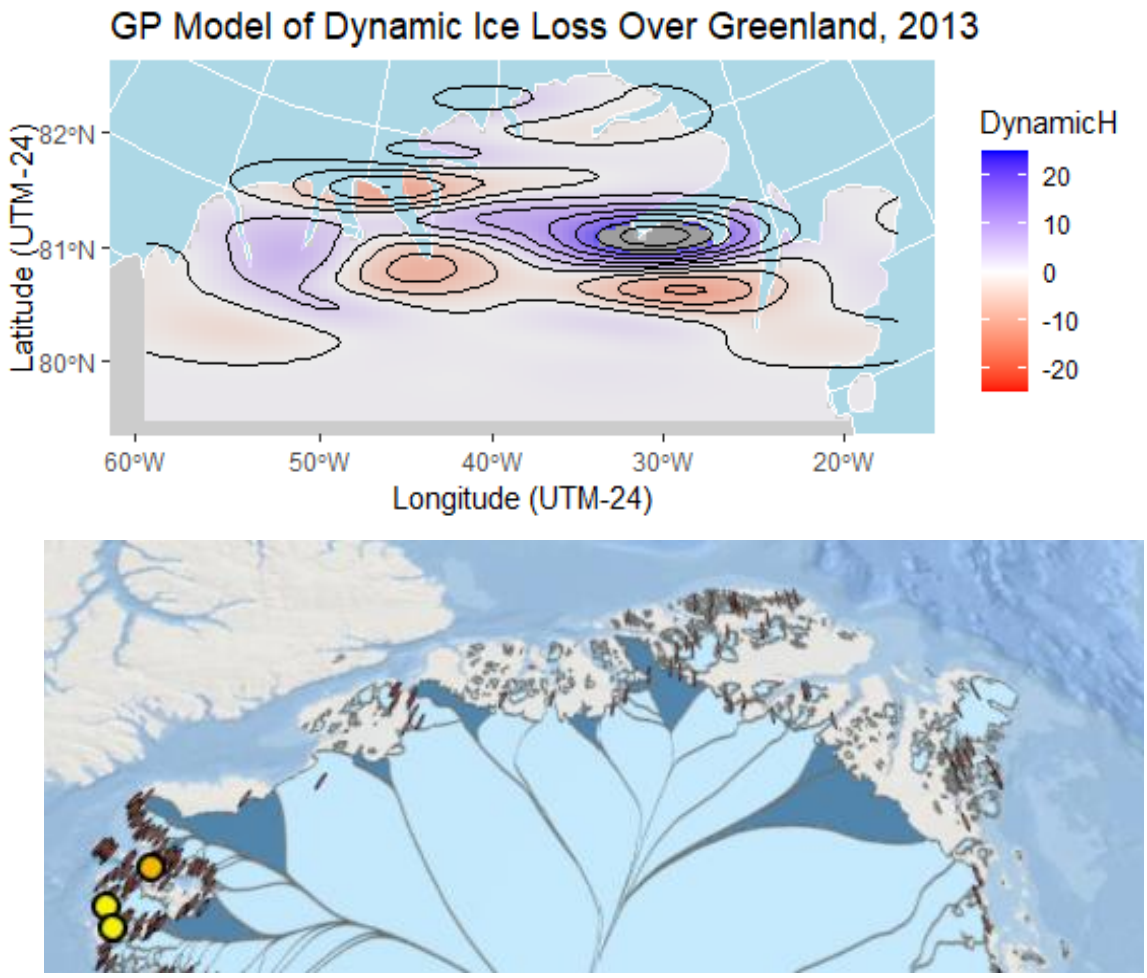

Figure 14. The top image is the Gaussian process model of dynamic ice loss in 2013, and the bottom image is the ice velocity data from the PROMICE project (Solgaard, et al., 2021). The data from the PROMICE project covers 2016 to 2021, so this specific model year is outside the range of the ice velocity data, the Csatho data is more sparse in those years, so these are the closest points of comparison. The ice velocity data is consistent with the catchment basin data in Figure 13 showing similar regions of high flow and low flow.

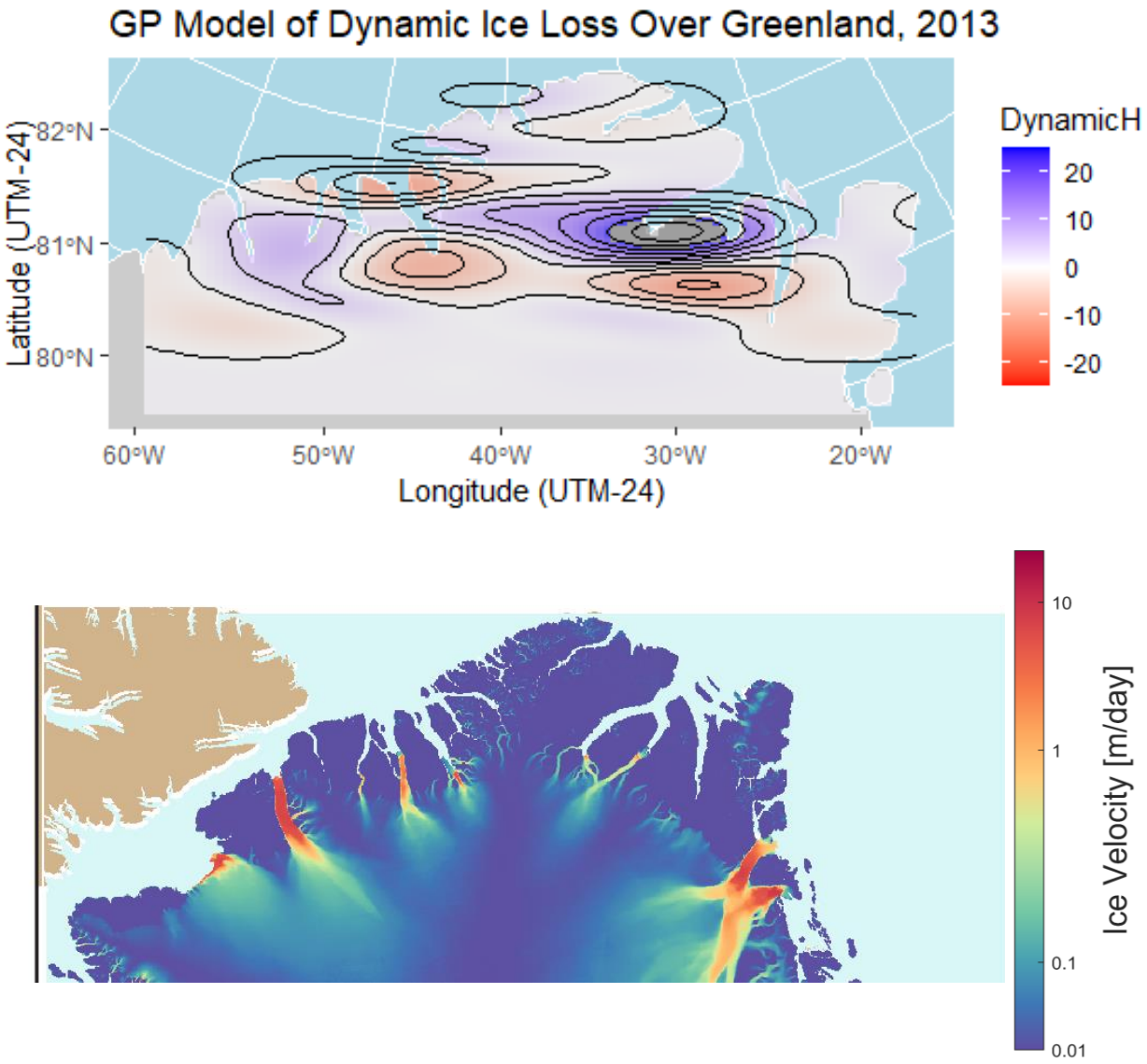

Uncertainty Analysis

Understanding the uncertainty in the model is an important component of the analysis that is complicated by the size of the dataset. Figure 15 shows an example of an uncertainty model from the {RobustGASP} package. The images shown are the Gaussian process model of the dynamic ice loss from a given year (in this case, 1999), and the error model from the same

year. The year 1999 had data from 5 of the 7 tiles (30-34) and was the largest set of values {RobustGASP} was able to process without dividing up the yearly datasets into smaller chunks. The result is typical of the results from other years with most of the region tending toward a large average uncertainty, and smaller values that are relatively local to the regions where observations were obtained. The data in this region is relatively sparse, compared to the number of observations in other tiles for more southern regions of the island, however, as with the more robustly sampled years such as 2003-2009, the number of observations is so large that the entire region cannot be modeled at once. 2003, for example, had over 11,000 observations, with two variables, requiring the inversion of a matrix 22,000 by 22,000 size matrix. Further work on the dataset will require the deployment of sampling methods or subsetting in order to obtain models and uncertainty estimates of the regions.

Implications and Discussion (and Literature Review)

The results of this analysis are somewhat mixed indicating a mixed relationship to elevation, and a suggestive relationship with drainage basins with higher flow, and high ice velocity rates. While unable to quantify the relationship in this analysis, this analysis does suggest that catchment basin and ice velocity data could serve as a check for error analysis and outlier analysis. Dynamic ice gain in regions of high flow rates would seem to be particularly unlikely, and therefore a good candidate for cleaning and removal. However, further analysis of the remainder of the Greenland ice sheet should be conducted to determine the robustness of this relationship, including focus on specific regions where ice loss is particularly acute.

Figure 15. This figure compares the Gaussian process model of dynamic ice loss in 1999 (from {kernlab}) with the Gaussian process model errors estimated from {RobustGASP}. This result is typical of other years that were able to be computed all at once, with the broad region receiving a high level of uncertainty that is larger than most of the predicted values in the range, with low errors locations to observation locations. Data collection locations are sufficiently spread out that most areas take on relatively high uncertainty values.

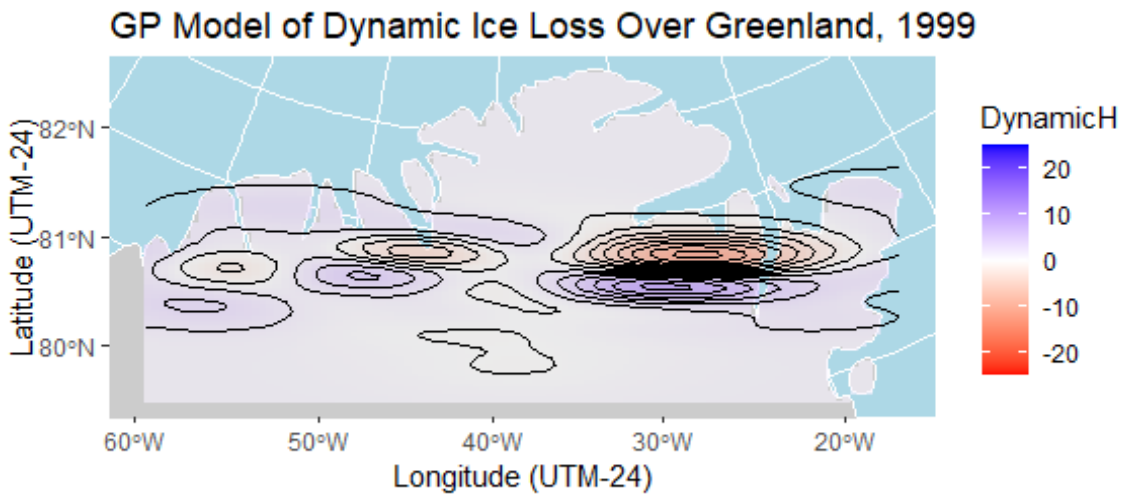

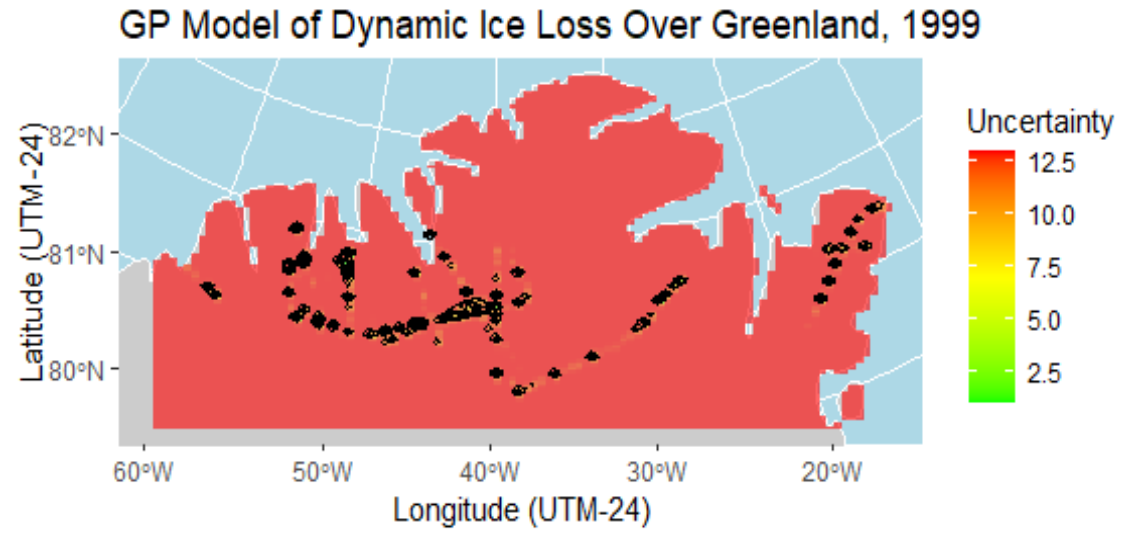

Modeling changes to the Greenland Ice Sheet (GrIS) can be quite challenging for a number of reasons related to its remoteness, challenging climate, satellite coverage and the

sparsity of available data. However, melting Greenland ice is expected to be a major driver of sea-level rise. Data can be obtained directly, or remotely, but then it must be validated if the data is to be of use in climate models. Understanding how various elements of the Greenland ice sheet system can be crucial to determining the accuracy of collected data, or which data may be used as a proxy when crucial data is missing.

The dynamics of the Greenland Ice Sheet (GrIS) have been a major focus in recent glaciological research, particularly due to the critical role the ice sheet plays in global sea level rise. This review synthesizes key findings from five studies that utilize satellite data and modeling to analyze ice loss, ice velocity, and the precision of data collection techniques.

Csatho et al. (2014) utilized laser altimetry data to reveal the spatial variability of ice thinning across Greenland. Their research emphasized that relying on data from a small number of outlet glaciers can lead to misleading conclusions about ice loss. Instead, their study, which uses data from 100,000 locations, provides a more accurate and spatially comprehensive estimate of ice sheet thinning. This regional variability in thinning rates is a key consideration for this project, especially as the available data set expands the time series and spatial resolution to 150,000 locations. The methodological framework from Csatho et al., (2014) including the use of LIDAR data for precise ice elevation measurements, is a foundation for this new analysis of Greenland's ice dynamics.

Solgaard et al. (2021) contribute to this research by focusing on ice velocity mapping, which provides insight into the movement of the ice sheet. Their study leverages synthetic aperture radar (SAR) data to improve the temporal and spatial resolution of velocity estimates, offering almost real-time updates on ice sheet dynamics. This work is relevant to this project as it provides a potential point of comparison for new ice loss models, particularly in exploring

whether dynamic ice loss correlates with increased ice velocities. Additionally, their methods for error estimation and smoothing are directly applicable to handling areas with uneven terrain, where errors in the dynamic ice loss dataset may need correction.

The study by Bolch et al. (2013) zooms in on the mass loss of Greenland's glaciers from 2003 to 2008, offering a narrower but highly relevant temporal focus. Their research highlights how climate forcing, especially temperature changes, directly influences glacier mass loss. This finding provides crucial context for the new analysis, as understanding the relationship between climate change and ice dynamics will help interpret the results of the new model. By considering how external climate forces drive ice loss, Bolch et al.'s study supports the broader narrative of accelerating ice loss in response to a warming climate.

In contrast, Goelzer et al. (2017) offers a broader perspective by reviewing recent advancements in ice sheet modeling, focusing on large-scale simulations and future projections. This article outlines key challenges and advancements in modeling ice dynamics, including data assimilation and the integration of high-resolution data products. These insights will be critical for refining these new modeling efforts, particularly when considering how to incorporate real-time data updates and adjust model parameters for greater accuracy.

Finally, Brenner et al. (2007) focuses on the precision and accuracy of satellite radar and laser altimeter data, which is crucial for evaluating the reliability of ice loss dataset. Their analysis of data collection techniques provides foundational knowledge for understanding the strengths and limitations of LIDAR data in measuring ice sheet elevation changes. This will be instrumental in assessing the quality of the dynamic ice loss data and guiding any necessary adjustments during analysis.

The results of this analysis are consistent with previous analyses of the Greenland ice sheet in that some areas are prone to greater ice loss than other regions. Given that the area of focus here is more limited, while other analyses in the literature, include Csatho, et al. (2014) covered the entire island, it is more difficult to place this analysis in the greater context. This region appears to be broadly speaking, relatively stable, and gaining, on average, a small amount of ice depth. Ice loss in other regions of the island could very well overwhelm the modest gains seen in this region of the ice sheet.

Conclusion

The main results of this analysis suggest that the laser altimetry data analyzed here should be taken in the context of other data and models available on the Greenland ice sheet. While there does appear to be a modest relationship with ice flow rates, further analysis is needed to determine the quantitative relationship between the two. Ice flow data may be useful for cleaning the data of outliers in a more robust fashion than the initial, conservative attempt here. Relationship with elevation appear to be more tenuous but should be further analyzed on a broader region of the ice sheet.

Improvement to the laser altimetry methods for ICESat-2 could also reduce the presence of some of the extreme outliers included in the present dataset. That data would also extend the timeframe of the data to produce better overlap with the PROMICE data to produce a more robust point of comparison.

Modeling the ice loss with LOESS is relatively easy and computationally less expensive than Gaussian process modelling, however, some additional analysis of the best span for each year is necessary to determine with best value to use. While Gaussian process regression is more

sensitive to the data locally, it is much more computationally expensive. Sampling or tiling will need to be done to model the ice sheet over large regions. This will be worth returning to in a future analysis that can include a larger portion of the ice sheet and tiles that are more dense with observations. Focus on specific regions, such as around interesting glacier outlets can also be undertaken. A small enough region could be interest to model spatial-temporally.

An early goal of this project was to obtain a numerical correlation with the elevation model and the dynamic ice loss model, and between the ice velocity model and the ice loss models. This is something that can be returned to in a future analysis.

References

Anjyo, K., & Lewis, J. P. (2011). RBF interpolation and Gaussian process regression through an RKHS formulation. *Journal of Math-for-Industry, 3*.

Applegate, P. J., Kirchner, N., Stone, E. J., Keller, K., & Greve, R. (2011). Preliminary assessment of model parametric uncertainty in projections of Greenland Ice Sheet behavior. *The Cryosphere Discussions*. doi:doi:10.5194/tcd-5-3175-2011

Bamber, J. L., Ekholm, S., & Krabill, W. B. (2001). A new, high-resolution digital elevation model of Greenland fully validated with airborne laser altimeter data. *JOURNAL OF GEOPHYSICAL RESEARCH, 106*.

Bjørk, A., Kruse, L., & Michaelsen, P. (2016). GreenlandGlacierNames_GGNv01. doi:https://doi.org/10.6084/m9.figshare.1449148.v2

Bolch, T., Sørensen, L. S., Simonsen, S. B., Mölg, N., & Machguth, H. (2013). Mass loss of Greenland's glaciers and ice caps 2003–2008 revealed from ICESat laser altimetry data. *GEOPHYSICAL RESEARCH LETTERS, 40*. doi:doi:10.1002/grl.50270

Csatho, B. M., Schenk, A. F., Veen, C. J., & Angelen, J. H. (2014). Laser altimetry reveals complex pattern of Greenland Ice Sheet dynamics. *Proceedings of the National Academy of Sciences, 11*(52), 18478-18483. doi:https://doi.org/10.1073/pnas.1411680112

Goelzer, H., Robinson, A., Seroussi, H., & deWal, R. S. (2017). Recent Progress in Greenland Ice Sheet Modelling. *GLACIOLOGY AND CLIMATE CHANGE*. doi:https://doi.org/10.1007/s40641-017-0073-y

Hugonnet, R., McNabb, R., Berthier, E., Menounos, B., Nuth, C., Girod, L., . . . Kääb, A. (2021). Accelerated global glacier mass loss in the early twenty-first century. *Nature*. doi:https://doi.org/10.1038/s41586-021-03436-z

Mouginot, J., & Rignot, E. (2019). Glacier catchments/basins for the Greenland Ice Sheet. doi:https://doi.org/10.7280/D1WT11

Pitcher, L. H., Smith, L. C., Gleason, C. J., & Yang, K. (2016). CryoSheds: a GIS modeling framework for delineating land-ice watersheds for the Greenland Ice Sheet. *GIScience & Remote Sensing*. doi:https://doi.org/10.1080/15481603.2016.1230084

Price, S. F., Hoffman, M. J., Bonin, J. A., Howat, I. M., Neumann, T., Saba, J., . . . al., e. (2017). An ice sheet model validation framework for the Greenland ice sheet. *Geoscientific Model Development, 10*. doi:doi:10.5194/gmd-10-255-2017

Rignot, E., Broeke, I. V., Monaghan, A., & Lenaerts, J. T. (2011). Acceleration of the contribution of the Greenland and Antarctic ice sheets to sea level rise. *GEOPHYSICAL RESEARCH LETTERS, 38*. doi:doi:10.1029/2011GL046583

Simonsen, S. B., Barletta, V. R., Colgan, W. T., & Sørensen, L. S. (2021). Greenland Ice Sheet Mass Balance (1992–2020) From Calibrated Radar Altimetry. *Geophysical Research Letters*. doi:10.1029/2020GL091216

Solgaard, A., Kusk, A., Boncori, J. P., Dall, J., Mankoff, K. D., Ahlstrøm, A. P., . . . Fausto, R. S. (2021). *Greenland ice velocity maps from the PROMICE project.* Retrieved from Earth System Science Data: https://essd.copernicus.org/articles/13/3491/2021/

Appendix.

Figure 1A. The image shows a map of Greenland with the ranges of the tiles that subset the Csatho, et al. (2014) dataset, numbered 1-36. The subset of data used in this analysis are selected from tiles 30-36 in the northern part of the island.

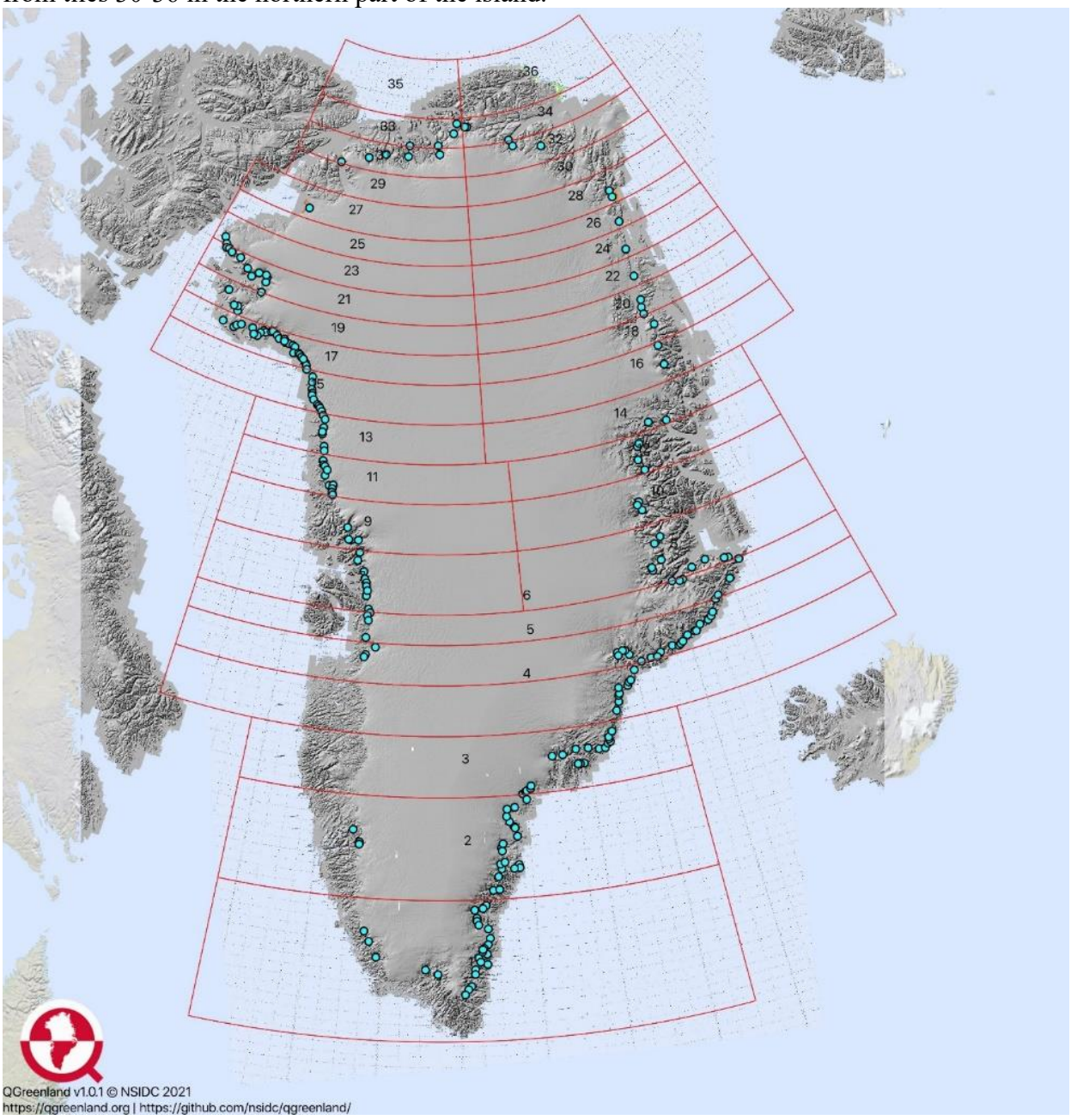

Figure 2A. The graph below shows the catchment basins and major outflow glaciers of Greenland. As indicated on the map, the northern part of the island has a lower concentration of major outflow glaciers (small brown dots). The areas in darker blue indicate areas of higher outflow of the drainage basins. A blue shading of any color indicates the extent of the ice sheet relative to the exposed landmass.

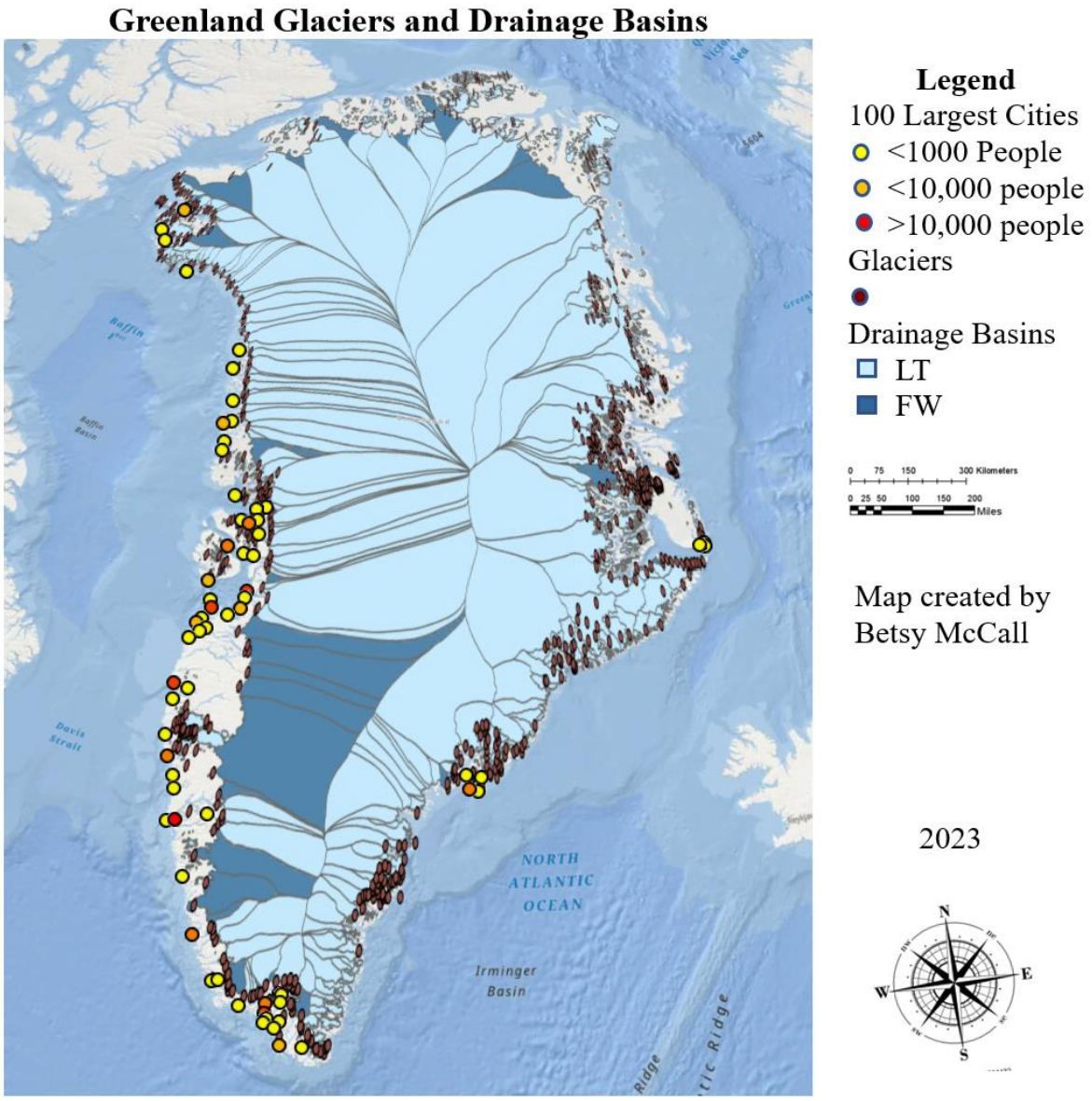

Data Sources:
ArcGIS
(Bjørk, Kruse, & Michaelsen, 2016)
(Mouginot & Rignot, 2019)
(Pareto Software, LLC Staff, 2023)

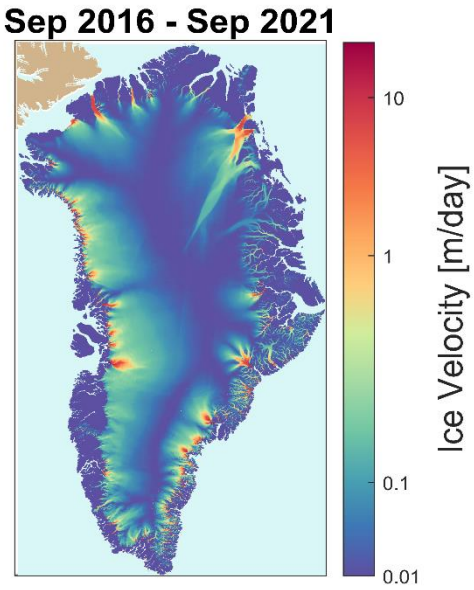

Figure 3A. This figure shows the ice velocity map from the PROMICE project. The data overlaps with the Csatho dataset only in the final year or so of that data, and the first year or so of this dataset. The full map is shown here. (Solgaard, et al., 2021)